PIER C

(Received 3 November 2024, Accepted 8 April 2025, Scheduled 17 April 2025)

Impact of Different Integration Times on Distributions of Rain Rates for Predictions of Rain Attenuation

Mohammad R. Hassan[1], Islam Md. Rafiqul[1,*], Mohamed H. Habaebi[1], Ahmad Z. Suriza[1], Khairayu Badron[1], Asma A. Budalal[2], and Md. M. H. Mahfuz[3]

[1]*Department of Electrical and Computer Engineering, Faculty of Engineering International Islamic University Malaysia, Jalan Gombak, Kuala Lumpur 53100, Malaysia*
[2]*College of Electrical and Electronics Technology, Benghazi, Libya*
[3]*Department of Electrical and Computer Engineering, Concordia University, Canada*

ABSTRACT: All wireless communication systems are moving towards higher and higher frequencies day by day which are severely attenuated by rains in outdoor environment. To design a reliable RF system, an accurate prediction method of rain attenuation is established and used globally based on local rain intensity measurement. Required rain intensity used for attenuation prediction is generally measured at a point with 1-min integration time or converted from higher integration time to 1-min. Recent measurements of rain intensity with a 10-second integration time indicate that intensity is not uniform over a 1-minute duration. Consequently, the statistics of rain intensity distribution and attenuation predictions are influenced by measurements with integration times shorter than 1 minute. It has been established that an integration time of 0.01% provides the optimal fit for actual rain rate data. This paper presents the rain intensity distributions from data measured with 2-min, 1-min, 30-sec, 20-sec, and 10-sec integration times, and it has impact on rain rate distributions as well as rain attenuation predictions.

1. INTRODUCTION

Various detrimental propagation processes affect mmWave communications, with rain attenuation being the most prominent. Attenuation prediction model is an essential tool for the design of satellite and terrestrial communication systems. The International Telecommunication Union-Radio (ITU-R) communication has proposed approaches for predicting rain attenuation. ITU-R P.530-18 provides propagation data and prediction techniques crucial for the design of terrestrial line-of-sight systems [1], whereas ITU-R P.618-14 offers propagation data and prediction methods required for the design of Earth-space communications systems [2]. Both prediction models recommend that rain intensity be evaluated with an integration period of one minute or fewer to correctly estimate its effects on microwave propagation. ITU-R P.837-7 [3] has proposed global rain rate statistics with a 1-minute integration period, employing the simulated motion of synthetic rain cells for the conversion of integration time. If rain rate information with longer integration time is available, ITU-R P.837-7 [3] has suggested a conversion technique to change data from a 5-minute integration time to a 60-minute integration time for the purpose of converting 1-minute integration time.

All predictive models need a rain rate at 0.01% of the occurrence duration, recorded using a rain gauge with a 1-minute integration period. Limited studies of rain attenuation from Earth-satellite linkages in Malaysia indicated that the ITU-R P.618-14 model overestimated the data at Ku-band [4]. Conversely, limited measurements of terrestrial connections under 1 km indicated that ITU-R P.530-18 overestimated values for Ka- and V-bands [5].

The National Climatic Centre provided short-duration rainfall data for around 250 sites in the U.S., detailing rainfalls that surpass a threshold determined by the rain-gauge integration time T. A "5-min rain rate" is the mean value of the fluctuating rain rate over a 5-minute period, computed as $\Delta H/T$, where ΔH denotes the total rainfall depth over 5 minutes, and $T = 5\,\text{min} = 1/12\,\text{h}$ is the integration time of the rain gauge. The investigation indicates that a reduced integration time enhances the resolution of rain rate in mm/hr [6].

A study of data from a network of four tipping bucket rain gauges in Singapore over four years has been performed to compute rainfall rate statistics utilizing integration times of 0.5, 1, 5, 10, 30, and 60 minutes. The rainfall rate was computed using a "variable integration time" or "instantaneous" approach. A rain rate of 12 mm/h is equivalent to a one-minute integration period, while a rain rate of 720 mm/h is equivalent to a one-second integration duration. It illustrated that measurements yielded increased rain rates when integration times were reduced. At a 1-minute interval, the rain rate is evidently 110 mm/hr; however, it is only 50 mm/hr at a 60-minute integration period for 0.01% of the time in a year. The research on instantaneous rain rate data suggests that these findings are consistent with one-minute statistics within a range of 0.01% to 1% of the time. However, they exhibit substantial discrepancies when the proportion of time falls below 0.01% or exceeds 1%. The lowest integration time utilized (i.e., the sampling rate

* Corresponding author: Islam Md. Rafiqul (rafiq@iium.edu.my).

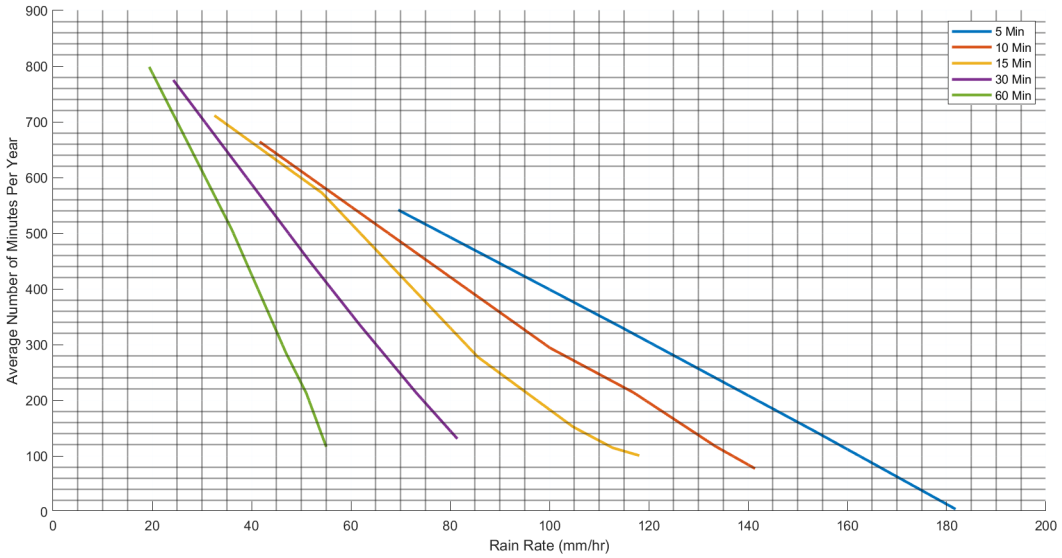

FIGURE 1. The rain rates distributions for 20-years measurement (1953–1972) in the New York metropolitan area.

or the precision of the recorded time for the rain event by the data recorder) substantially influences the statistics of rainfall rate with varying integration times in Singapore, due to the elevated rainfall rates. This is particularly true for high rainfall rates that occur for less than 0.01% of the time [7].

Distributions of rainfall rates with integration times of 1, 10, 20, 30, and 60 minutes were analyzed based on two years of rain-rate data done by ETRI Lab in Korea. To get a dependable 1-minute rain rate distribution, it is essential to employ an efficient approach for converting data from various integration times to a 1-minute rain rate distribution. It was evident that shorter integration times yield elevated rainfall rates from the measurement [8].

All observations clearly indicate that a shorter integration period results in improved resolution of rain rate in mm/hr and yields greater rain rates from the readings. No observations exist for integration durations less than one minute, and the effects on rain rate statistics and rain attenuation predictions for reduced integration times have not been thoroughly examined. This article delineates the statistical distributions of rain rate recorded in Malaysia utilizing integration durations of 10 seconds, 20 seconds, 30 seconds, 1 minute, and 2 minutes. Rain rate data are calculated for five integration durations and compared with ITU-R P.837-7 and Global Moupfouma models, which are predicated on a 1-minute integration duration. The ITU-R P.530-18 prediction technique estimates rain attenuation in terrestrial links using observed rain rates with integration times of 10 seconds, 20 seconds, 30 seconds, 1 minute, and 2 minutes, then compares the results with actual observations.

2. RAIN RATE MEASUREMENTS WITH MULTIPLE INTEGRATION TIMES

Meteorological services have tracked rainfall intensity with an integration time of one hour or longer for several decades. The rain rate distribution depends on the integration time of rain gauges, as initially articulated by Lin in the Bell System Journal in 1976 [6]. Subsequently, several researches have uncovered the risks in the following years, which are outlined in this section. Rain intensities for microwave propagation and effect analysis were recorded with integration lengths of 1, 5, 10, 30, and 60 minutes, and are detailed in the following sections.

2.1. National Climatic Center Measurement [6]

The National Climatic Center supplied short-duration rainfall data for around 250 locations in the U.S., specifying rainfalls that exceed a threshold established by the rain-gauge integration time T. The thresholds are 76 mm/h for $T = 5$ minutes and 20 mm/h for $T = 60$ minutes. This article outlines a methodology for extracting 5-minute precipitation rate distributions from extensive datasets (≥ 20 years).

In his research, Lin defined the "5-minute rain rate" as the mean value of the stochastic rain rate over a 5-minute interval, calculated as $\Delta H/T$. Here, ΔH represents the cumulative rainfall depth over 5 minutes, and $T = 5\,\text{min} = 1/12\,\text{h}$ denotes the integration duration of the rain gauge. As illustrated in Fig. 1, a "T-min rain rate" denotes the average precipitation rate over a T-minute period. The investigation suggests that the resolution of the rain rate in mm/hr is improved by a shorter integration time.

2.2. Singapore Measurement [7]

The research analyzed data from a network of four tipping bucket rain gauges in Singapore over four years to calculate rainfall rate statistics at various integration intervals of 0.5, 1, 5, 10, 30, and 60 minutes. Ong and Zhu [7] employed the "instantaneous" or variable integration time computing method for evaluating rainfall rates. The variable integration time Δt (interval between tips) for a 0.2 mm tipping container size is established as follows:

$$R = 3600 * \frac{0.2}{\Delta t} = \frac{720}{\Delta t}\ \text{mm/hr} \tag{1}$$

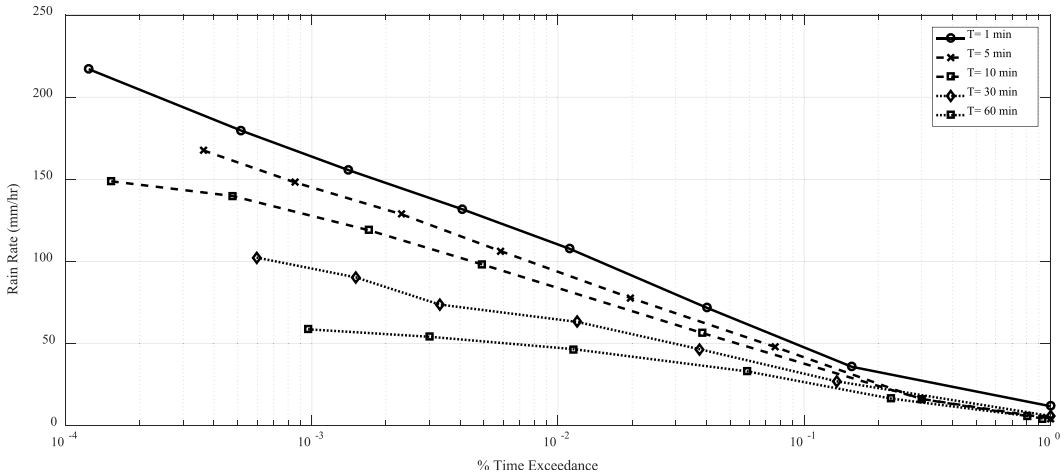

FIGURE 2. Rainfall rates with integration durations of 1, 5, 10, 30, and 60 minutes recorded in Singapore [7].

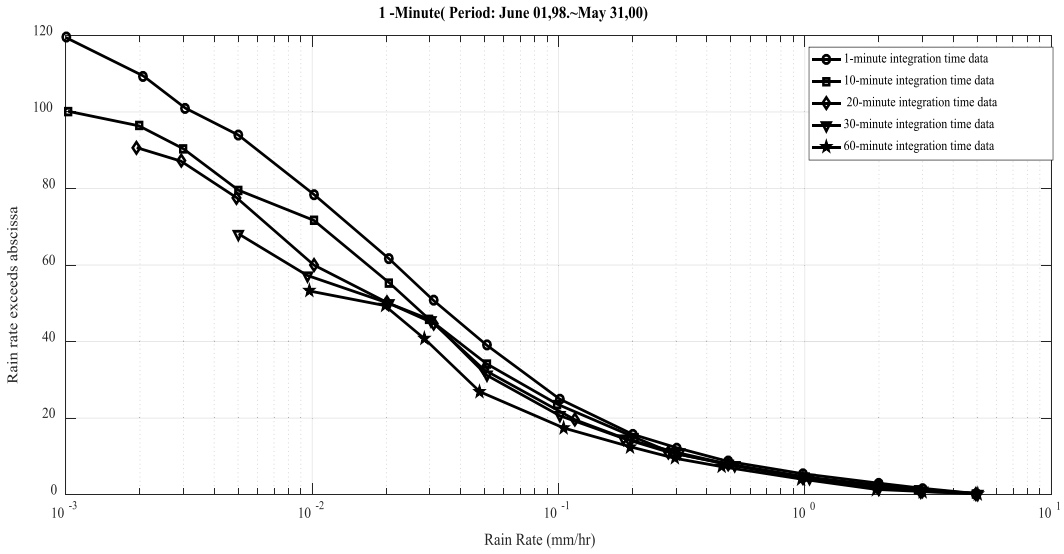

FIGURE 3. Rain rate distributions derived from two years of measurements in Korea, utilizing data with varying integration times [8].

where R is the rain rate in millimeters per hour, and Δt is expressed in seconds. It has been observed that a rain rate of 12 mm/h is equivalent to a 1 minute integration time, while a 1 second integration time is equivalent to a 720 mm/h rain rate.

It is evident from Fig. 2 that the rain rates are higher when the integration time is short. It is evident that the rain rate is 110 mm/hr at a 1-minute interval, but it is only 50 mm/hr at a 60-minute integration period for 0.01% of the year. These results are consistent with the one-minute statistics within a range of 0.01% to 1% of time, according to the research on instantaneous rain rate statistics. However, a notable divergence arises when the proportion of time is either below 0.01% or exceeds 1%. The minimum integration time utilized in Singapore significantly affects the rainfall rate data with varying integration times. The duration is dictated by the sampling rate or the precision of the recorded time for the rain event by the data recorder. This is a consequence of the increased precipitation levels that we encounter. It is particularly accurate when precipitation rates constantly surpass 0.01%. The sampling rate of one sample every 2 seconds may be inadequate for measuring a high rainfall rate beyond 180 mm/hr with a 0.2 mm tipping bucket size. Further extensive studies are required to assess the impact of variables such as disposal container dimensions, rain gauge collection aperture, and sample frequency on rainfall rate statistics for different integration durations in regions with high precipitation rates. The results diverged from those of others, who indicated negligible disparities between the rain rate statistics derived via variable integration time and those acquired using a one-minute interval. Tropical places, such as Singapore, may have much higher rainfall rates than temperate regions.

2.3. ETRI Lab Measurement [8, 9]

The distributions of rainfall rate with 1-, 10-, 20-, 30-, and 60-minute integration times are analyzed and illustrated in Fig. 3, based on 2-year rain-rate measurements conducted by Lee et al. at ETRI Lab in Korea [8]. Obtaining rain rate data with a 1-minute integration time for a period of 10 years in Korea is a challenging task. It is essential to employ an effective method to convert from other integration time data to a 1-minute rain

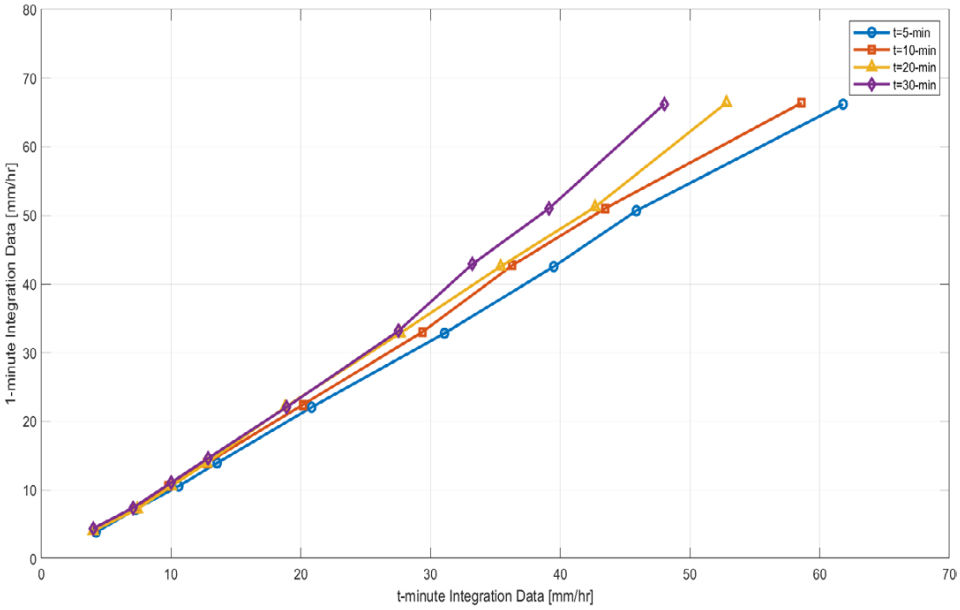

FIGURE 4. In Korea, an equal-probability relationship was observed between rain rate data with varying integration times [9].

rate distribution in order to ensure the reliability of the distribution. It is evident from Fig. 3 that the rain rates are higher when the integration time is short.

It is advised that the distribution be inferred from observed rainfall data with an integration time of 1 minute or less, as demonstrated in another measurement conducted in the ETRI Lab by Jung et al. [9]. The analysis and presentation of Fig. 4 are based on six years of measurement in various locations. It demonstrates the same behavior as previously observed, indicating that a shorter integration time results in higher rain rates from the measurement.

2.4. Measurement by Japan Meteorological Agency [10]

Fukuchi [10] reported a 7-year measurement in Japan by the Japan Meteorological Agency, which included data at 5-minute intervals and approximately 1 km mesh points. Acquiring rain data with such a brief time integration is a challenging task. Then, it is highly beneficial to derive the spatial correlation of the rainfall rate integration time dependence. This knowledge allows us to assess the effective spatial correlation with a short time integration of the rainfall rate. This study examines the time dependence of spatial correlation of rainfall rate using radar observations over Japan. The spatial correlation values at identical distances augment with prolonged integration time. This feature may emerge from the movement of the precipitation zone [10].

3. RAIN RATE DISTRIBUTION

Precipitation is an obstacle for higher frequency bands, particularly in tropical locations, where substantial precipitation with diverse characteristics is hazardous. Rain attenuation poses a significant challenge in the construction of reliable networks inside the Ka- and V-bands, which represent the future trajectory of satellite communication systems. Consequently, a discussion of rain rate time series for estimating attenuation caused by rain in the context of fade mitigation is essential [11]. Diverse predictive methodologies are employed to assess rain attenuation. The bulk of these models, including those provided by Moupfouma [12], ITU-R [11], Crane [17], and Rice and Holmberg [19], are based on applied mathematical principles about rain rate.

3.1. Global Moupfouma Model [12--14]

The Moupfouma model accounts for the Rain Rate Time Series Behavior. The model is predicated on the cumulative distribution function of the rainfall rate. It is shown in Fig. 5. The model's equations (2)–(4) are employed using the $R_{0.01}$ percent value, obtained from a one-year measurement utilizing a 1-minute rain rate time series.

$$P\left(R \geq r\right) = \left(\frac{R_{0.01}+1}{r+1}\right)^{b} \times e^{[u\times(R_{0.01}-r)]-\log_e\left(10^4\right)} \quad (2)$$

The variable r represents the fraction of the exceeded rain rate, whereas b denotes the Cumulative Distribution Function (CDF) of the rainfall rate, as seen in Equation (3):

$$b = \left(\frac{r-R_{0.01}}{R_{0.01}}\right) \times \log_e\left(1+\frac{r}{R_{0.01}}\right) \quad (3)$$

Parameter u is defined as the slope of cumulative rainfall distributions and represented by the following Equation (4), pertinent to the local meteorological circumstances and geographical characteristics.

$$u = \frac{\log_e\left(10^4\right)}{R_{0.01}} \times e^{-\lambda\times(r/R_{0.01})\gamma} \quad (4)$$

Here, λ and γ as positive constants are defined for tropical and equatorial climate, where $\lambda = 1.066$ and $\gamma = 0.214$.

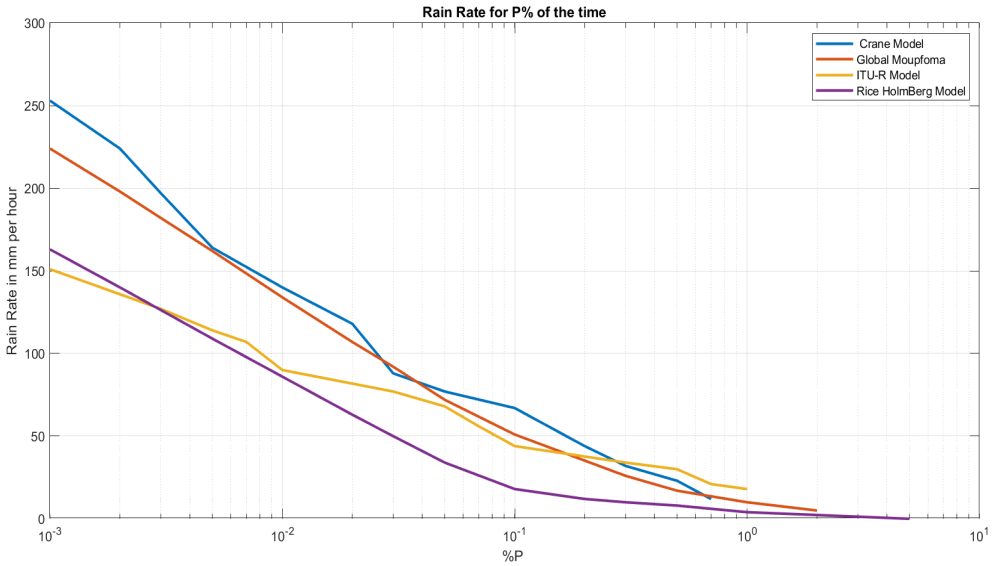

FIGURE 5. Comparison among the rain rate distribution predicted by Global Moupfouma, ITU-R, Rice-Holmberg and Crane model.

3.2. Modified Moupfouma Rain Rate Distribution Model [15]

Chebil's model is appropriate for estimating $R_{0.01}$ and permits the use of long-term mean yearly accumulation, M, at the site [16]. The model's power law is expressed as

$$R_{0.01} = \alpha M^{\beta} \tag{5}$$

α and β are the regression coefficients. Chebil and Rahman have conducted a comparison of several models utilizing measured values of $R_{0.01}$ and M in Malaysia, Indonesia, Brazil, Singapore, and Vietnam. They demonstrated that their model is the most accurate representation of the measured data [16]. The regression coefficients α and β are defined as follows.

$$\alpha = 12.2903 \quad \text{and} \quad \beta = 0.2973$$

In modified Moupfouma, the equation employed resembles that of the global Moupfouma [12].

3.3. ITU-R Model [11]

It is employed in the ITU-R model [11] to compute the rain rate for a particular site based on its geographic coordinates. For p percent of the typical year, the rainfall rate, R_p, was surpassed, where p is P_0, in line with Equation (6). It is presented in Fig. 5.

$$R_p = \frac{-B + \sqrt{B^2 - 4AC}}{2A} \text{ mm/hr} \tag{6}$$

$$A = ab$$
$$B = a + c\ln(p/P_0(Lat, Lon))$$
$$C = \ln(p/P_0(Lat, Lon))$$

3.4. Crane Model [17, 18]

The precipitation climatic zone for Crane's model must be established utilizing his global model. Crane [17] has presented a Global Model capable of estimating point rain rates, variations in rain rates along a path, and height, utilizing data from geophysical sources. The model can deliver the rain rate in point form at the surface or as a percentage of the annual duration during which the attenuation threshold is exceeded.

The Crane's global model is initially employed to delineate the precipitation climatic zone. This investigation, utilizing data from IIUM, concentrates on the H-region, encompassing Malaysia, with the rain rate distribution illustrated in Fig. 5.

3.5. Rice-Holmberg Model [19--21]

Based on local weather data, the model suggested by Rice and Holmberg [19] is used to guess how the rain rates will be spread out. The weather data came from the area data in a static form. For designing a communication system that works with what is available in the area, information on rain rates is needed for the rain-rate distribution model. Fig. 5 shows an example of how the rate of rain can change based on the climate in the area.

4. RAIN RATE DATA COLLECTION AND PROCESSING

Rain intensity data was gathered utilizing a Casella automated rain gauge, which was mounted on the rooftop of Block E2 at the Faculty of Engineering, IIUM Gombak Campus. The Casella rain gauge can capture rainfall rate data every 10 seconds with an accuracy of 0.2 mm. To guarantee unobstructed data gathering, it was positioned on a horizontal surface in an open space. Furthermore, the battery underwent regular testing to guarantee the continuous functionality of the data recording device. Table 1 displays the precise specifications, which encompass precision and tangible dimensions. The weight of the water causes it to overturn and release its contents. The measurement of rainfall volume and intensity over time is made possible by the establishment of an electrical contact with each container tip. The accumulated rain rate data was analyzed over two distinct time periods: from March 1, 2019 to February 29, 2020, and from August 1, 2022 to July 31, 2023.

TABLE 1. Real-time rain gauge type: Tipping bucket manufactured by Casella — Specifications.

bucket	0.20 mm
Shutter Area	400.0 cm^2
Authenticity	±2% at 1 litre/hour
Quantity	Unlimited
Signal generator	Magnet or Reed switch
Temperature range of operation	From 1°C to 85°C
Weight	2.6 kg

4.1. Transforming 10-Second Integration Time Data into Longer Period

The analysis of the rain rate data requires mathematical computations. By aggregating the data over a longer time frame, data with a lower integration time (less than 10 seconds) may be easily turned into data with a higher integration time. The data acquired at 10-second integration intervals are transformed to larger durations, such as 20 seconds, 30 seconds, 1 minute, and 2 minutes, using Equation (7). However, the attenuation prediction model does not work with data reported in millimeters per second, minute, or two minutes. As a result, we need to use Equation (8) to convert the values to mm/hour. All data acquired with 10-second integration intervals were converted to longer integration periods using Equations (7)–(8) [22]:

$$r_\tau = \sum_{k=t_i}^{t_f} r_k \tag{7}$$

where,

r_k = water-volume collected during rain at a specific time k

r_τ = accumulation of volume of rain for τ = 10 s, 20 s, 30 s, 1 min, 2 min, etc.

t_i = Rain starting time

t_f = Rain ending time

The rain rate is expressed in mm/hr, and R (mm/hr) can be obtained using Equation (8) as follows:

$$R = r_\tau T_\tau \tag{8}$$

$$T_\tau = \begin{cases} 360, & \tau = 10\,\text{sec} \\ 180, & \tau = 20\,\text{sec} \\ 120, & \tau = 30\,\text{sec} \\ 60, & \tau = 1\,\text{min} \\ 30, & \tau = 2\,\text{min} \end{cases}$$

The collected data at 10-sec integration time and converted to 20-sec, 30-sec, 1-min, and 2-min of a raining event occurring on August 1, 2022 are plotted in time domain and presented in Fig. 6. Fig. 6 illustrates the rain rate in mm/hr for five integration times for a half an hour period. It is obvious that the rain intensity is not uniform over 10-sec duration, hence it will keep reducing the intensity with longer than 10-sec integration. The rain rate in mm/hr displays lower values when the integration is performed with longer time. The peak rain intensities are observed at 144, 144, 120, 108, and 102 mm/hr with the integration times varied from 10 seconds, 20 seconds, 30 seconds, 1 minute, and 2 minutes. Obviously, integration times will affect the distribution statistics over longer periods also.

5. RESULTS AND ANALYSIS

5.1. Effects on Rain Rate Distributions

With the natural fluctuations in tropical precipitation, the behavior of radio communication networks is likely to exhibit a wide range of time-scales as well [23]. Equations (7)–(8) are used to estimate complementary cumulative distribution functions (CCDFs) from the recorded two-year rain rates with 10-sec integration durations. The results are shown in Fig. 7.

In Fig. 7, it is readily seen that the CCDF with shorter integration times displays a higher rain rate than that with longer integration durations. A comparison of 1 min integration rain rate with four integration times of 2 minutes, 30 seconds, 20 seconds, and 10 seconds is discussed below. The rain rate variations at 0.1%, 0.01%, and 0.001% of exceedance are calculated using Equation (9) and presented in Table 2.

$$\text{Variations} = \frac{\begin{pmatrix}\text{RAIN RATE}_{1\text{ Min integration of time at x\%}} \\ \sim \text{RAINRATE}_{\tau\text{ Minutes integration time at x\%}}\end{pmatrix}}{\text{RAIN RATE}_{1\text{ Min integration of time at x\%}}} \times 100\% \tag{9}$$

The precipitation rates are 85, 91, 97, 106, and 130 mm/hr, recorded over durations of 2 minutes, 1 minute, 30 seconds, 20 seconds, and 10 seconds, respectively, at a rate of 0.01%. Thus, the precipitation rate statistics with shorter integration intervals provide significantly higher values than those with extended integration durations. The $R_{0.01\%}$ value with a 10-second integration is approximately 43% more than that with a 1-minute integration period. The disparities escalate to 100% and 19.3% for rain rates of $R_{0.1\%}$ and $R_{0.001\%}$ for the 2022–2023 measurements. The $R_{0.01\%}$ value with a 10-second integration period is 54.2% more than that with a 1-minute integration duration. The disparities escalate to 169% and 56.6% for rain rates of $R_{0.1\%}$ and $R_{0.001\%}$ for the 2019–2020 measurements. The rain rate distribution data collected at IIUM Campus, utilizing a 10-second integration time and subsequently converted to 20 seconds, 30 seconds, 1 minute, and 2 minutes over a one-year duration, are analyzed to forecast rain intensity. This analysis employs the prediction models from ITU-R 837-7 [3] and Global Moupfouma [22], as illustrated in Fig. 8.

The ITU-R model's prediction is closed with one-minute integration time measurement. Moupfouma model performs suitably well [12], and the Global Moupfouma is closed with a 10-second integration time measurement at 0.01% outage. However, both rain rate distribution models are based on 1-minute rain intensity measurements.

5.2. Effects on Rain Attenuation Prediction

While the ITU-R model does a poor job of estimating terrestrial rain attenuation in tropical Malaysia, and the results of the tests

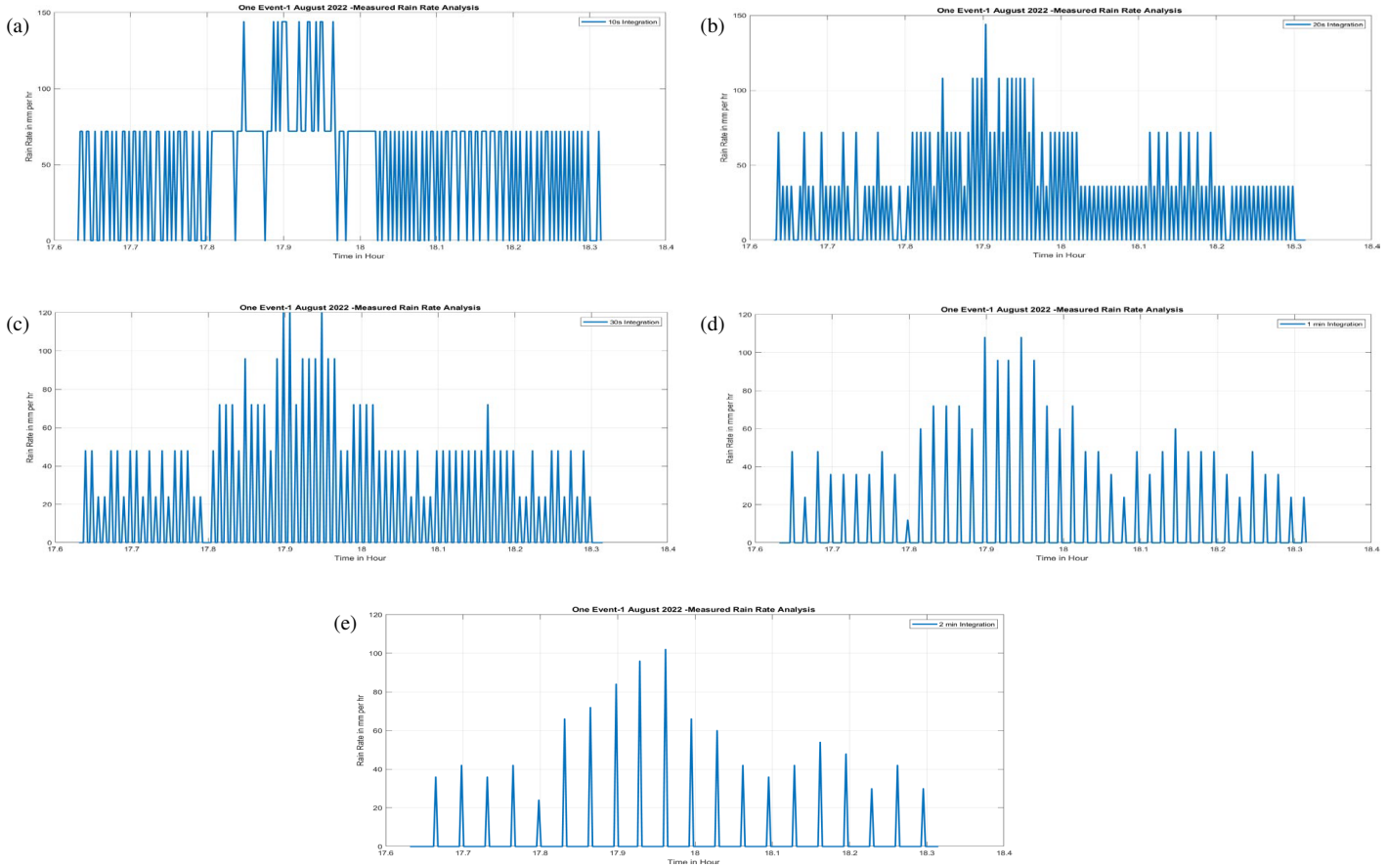

FIGURE 6. A real-time event of rain rate fluctuation was recorded on August 1, 2022, with integration times of (a) 10 seconds, (b) 20 seconds, (c) 30 seconds, (d) 1 minute, and (e) 2 minutes.

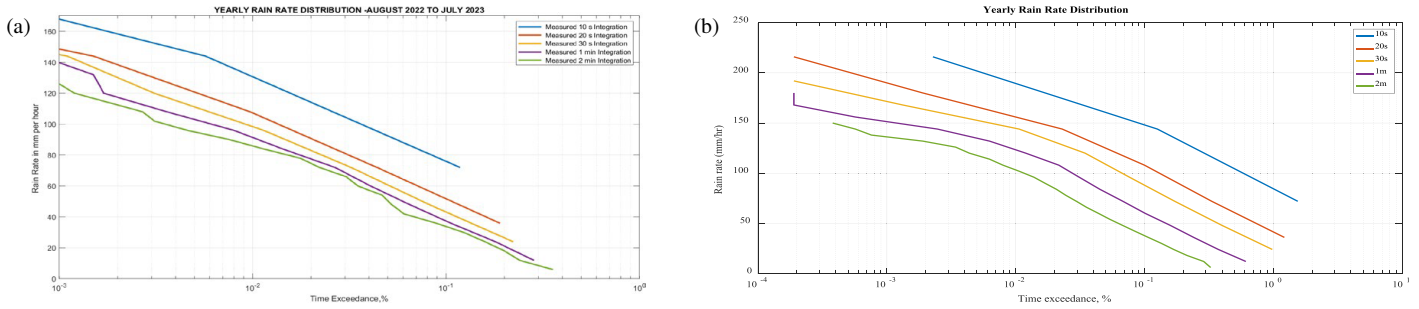

FIGURE 7. The complementary cumulative distribution functions by rain rates with five integration times measured in (a) 2022–2023 and (b) 2019–2020.

TABLE 2. Comparison of rain rate variations at τ integration times with 1 min integration of time at different % of exceedances.

	2022–2023		2019–2020		2022–2023		2019–2020		2022–2023		2019–2020	
Time	$R_{0.001\%}$ mm/hr	Var	$R_{0.001\%}$ mm/hr	Var	$R_{0.01\%}$ mm/hr	Var	$R_{0.01\%}$ mm/hr	Var	$R_{0.1\%}$ mm/hr	Var	$R_{0.1\%}$ mm/hr	Var
2-min	125	10.7%	143	5.9%	85	6.6%	100	16.7%	33	13.2%	42	23.6%
1-min	140	0%	152	0%	91	0%	120	0%	38	0%	55	0%
30 sec	144	2.9%	165	8.6%	97	6.6%	140	16.7%	43	13.2%	92	67.3%
20 sec	148	5.7%	191	25.7%	106	16.5%	155	29.2%	52	36.9%	104	89%
10 sec	167	19.3%	238	56.6%	130	43%	185	54.2%	76	100%	148	169%

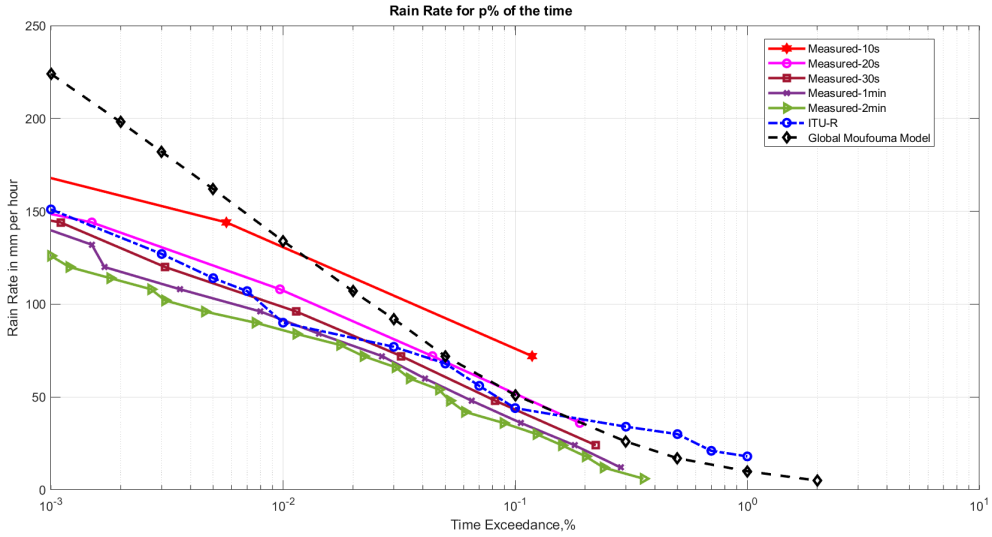

FIGURE 8. Comparison of the forecasted 1-minute rain rate using ITU-R P.837-7 and Global Moupfouma models with the measured rain rate with integration times of 10 seconds, 20 seconds, 30 seconds, 1 minute, and 2 minutes.

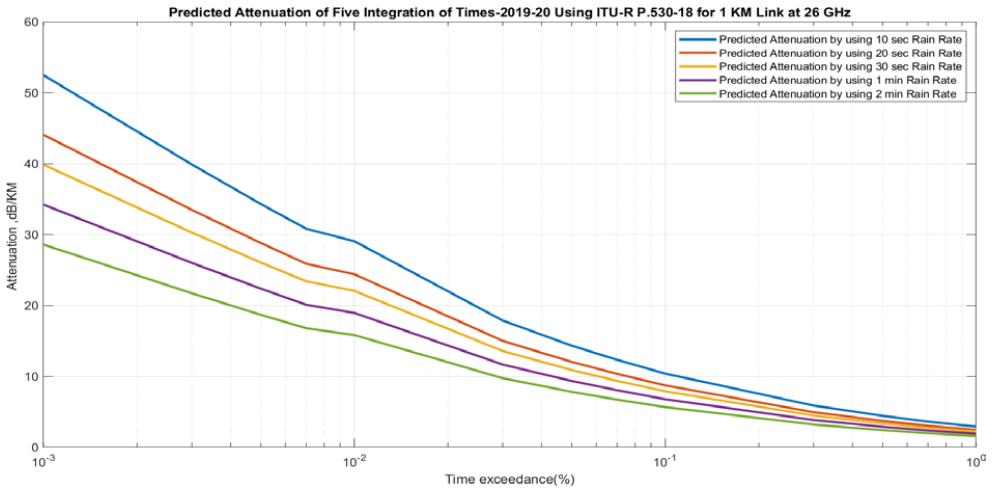

FIGURE 9. The predicted rain attenuations using measured rain rate with integration times of 10-sec, 20-sec, 30-sec, 1-min and 2-min based on ITU-R P.530-18.

show that it is the best option [25, 26]. In order to anticipate rain fade more often than 0.01%, the following formula was suggested for terrestrial microwave connection design in ITU-R P.530-18 [1, 27].

The precise rain attenuation, accounting for consistent fluctuations in rain intensity along a 1 kilometre course is delineated as follows:

$$\gamma\left(\frac{\text{dB}}{\text{km}}\right) = kR_{0.01\%}^{\alpha} \tag{10}$$

where $R_{0.01}$ = the real time rain rate mm/hour at 0.01%. Regression coefficients are k and α which relies on frequency and polarizations.

The total rain attenuation for the path length d kilometer is recommended as

$$A_{0.01} = \gamma d_{eff} = \gamma dr\,(\text{dB}) \tag{11}$$

where γ, dB/km, particular rain attenuation, d_{eff} = the effective path length in kilometre, d = actual path length in kilometre, r = distance factor as defined in Equation (12).

k and α are referred to as regression coefficients, with values obtainable from ITU P.838-3 [28]. Variable d denotes the path length (km), while r is defined as the reduction factor (distance factor) as specified in Equation (12).

$$r = \frac{1}{0.477d^{0.633}R_{0.01}^{0.073\cdot\alpha}f^{0.123} - 10.579(1-\exp(-0.024d))} \tag{12}$$

Using measured rain rates for different integration times for the year of 2022–2023 at 0.01% and Equation (5), the attenuations are predicted for 1 km path length and shown in Fig. 9. The predicted attenuation is 10 dB higher at 10-sec than 1-min integration time at 0.01% and almost 20 dB higher at 0.001%. It is shown very clearly that the rain attenuation predictions is di-

TABLE 3. Measured rain rates at 5 integration times projected using 1-min integration time at 0.01% of exceedances.

Integration of Time	Measured Rain Rate at 0.01% for 2022–2023	Projected Rain Rate at 0.01% for 2022–2023	Measured Rain Rate at 0.01% for 2019–2020	Projected Rain Rate at 0.01% for 2019–2020
10 s	130	166	185	179
20 s	106	135	155	150
30 s	97	124	140	135
1-min	91	116	120	116
2-min	85	108	100	97

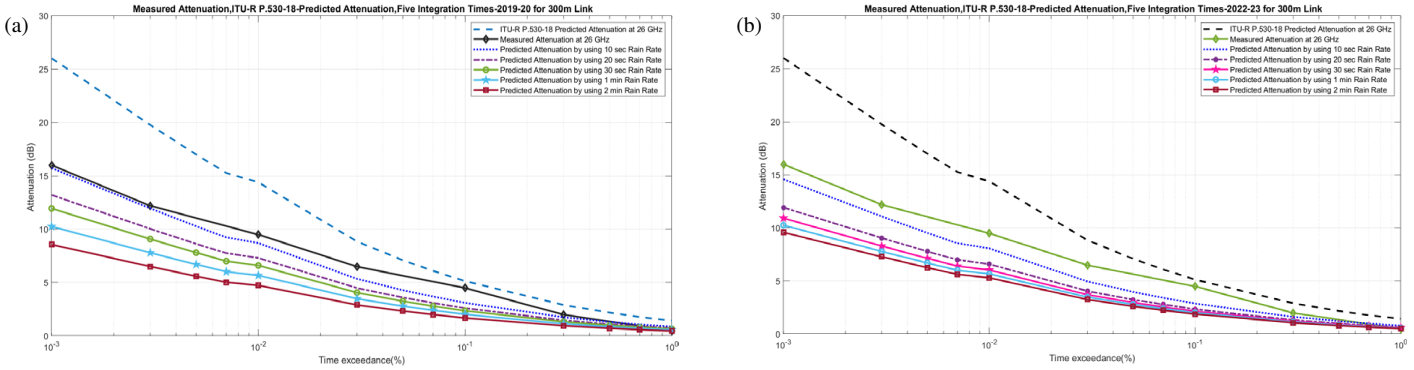

FIGURE 10. Comparison among predicted rain attenuations using ITU-R P.530-18 with 1 minute rain rate , those predicted using ITU-R P.530-18 with 5 integration times rain rates assuming reduction factor , $r = 1$ for (a) 2019–2020 and (b) 2022–2023 as well as measured at 26 GHz with 300 m length.

rectly related to 0.01% rain rate statistics which is higher with integration times less than 1 minute.

At the University Technology Malaysia (UTM), researchers spent a year measuring the impact of rain on a 26 GHz microwave link spanning 300 meters. Officially, 0.01% of the precipitation fell at a rate of 116 mm/hr [14]. In Equations (10)–(12), the ITU-R presented the now-universally-recognized dB/km rain attenuation formula. The model is employed to 'average out' the spatial in homogeneity of rain rate, uniformly distributed throughout a 1 km propagation channel, known as specific attenuation [28]. Equation (13) was used for extraction using a reference rain rate of 116 mm/hr [27], and the rain rate recorded over two years at various integration times is taken from Table 2. The projected rain rates using five different integration times are shown in Table 3.

$$\text{Projected Rain Rate}_{\text{Integration Time},\,\tau} = \left(\frac{116}{\text{Rain Rate}_{1-\text{min integration time}}}\right) \times \text{Integration Time},\tau \quad (13)$$

The effective path length is multiple times longer than the true journey length when the path length is less than 1 km, and the reduction factor r in Equation (12) gets more than 2. To compare the measured rain attenuation for a 300 m link length operating at 26 GHz frequency with the ITU-R P.530-18 forecast, Equations (10)–(12) were used. The results are displayed in Fig. 10. Equations (10)–(11) assume that the rain intensity is uniform throughout a 1 km route and use the recorded $R_{0.01}\%$ mm/hr to extrapolate for 10-, 20-, 30-, 1-, and 2-minute integration durations. Fig. 10 shows the comparison between the 26 GHz measurements and the projections made for a 300 m route length.

Using a $R_{0.01}\% = 116$ mm/hr with a measured 1-min integration time, the anticipated rain attenuation by ITU-R P.530-18 is substantially greater than the measurement, as shown in Fig. 10. The explanation for this is rather clear: when $d = 0.3$ km, the true path length in Equation (11) is many times less than the effective path length ($r = 2.54$) in Equation (12). Equations (10)–(12) assume a uniform and homogeneous distribution of rain intensity along a 1 km path; with a reduction factor $r = 1$, the prediction using $R_{0.01}\% = 116$ mm/hr with a 1-min integration time is significantly lower than measurement; however, $R_{0.01}\% = 179$ mm/hr and 166 mm/hr with 10-sec integration times are very close to measurements. For propagation paths longer than 1 km, the ITU-R model's 1-minute integration time may be sufficient to "average out" the spatial inhomogeneity of the rain rate; however, for shorter propagation paths, the rain intensity with lower integration times reflects more accurate predictions.

6. CONCLUSIONS

Rain fade is the principal challenge in the design of microwave devices functioning at high frequencies in tropical regions. All rain attenuation prediction models utilized rain intensity data with a 1-minute integration interval. Rain intensity data collected over a two-year period in Malaysia, with a 10-second integration interval, were converted to 20-second, 30-second, 1-minute, and 2-minute integration intervals to analyze the effect of integration time on rain rate distributions. Rainfall rates over

a 10-second integration period are 50% higher than those over a 1-minute interval with an outage rate of 0.01%. A 300 m microwave link operating at 26 GHz is predicted using the ITU-R P. series.530-18 prediction model, and the results are compared with actual measurements. In comparison to data collected over one year period with 5 integration times, the $R_{0.01}$% value, which is derived from a 10-second integration interval, is capable of more accurately predicting the observed attenuation. As a result, rain attenuation for short paths remains consistent for brief intervals and can be accurately predicted by rain rate measurements with an integration time of less than one minute.

REFERENCES

[1] ITU-R P.530-18, "Propagation data and prediction methods required for the design of terrestrial line-of-sight systems," Sep. 2021.

[2] ITU-R P.618-14, "Propagation data and prediction methods required for the design of Earth-space telecommunication systems," Aug. 2023.

[3] ITU-R P.837-7, "Characteristic of precipitation for propagation model," Jun. 2017.

[4] Ismail, A. F. and P. A. Watson, "Characteristics of fading and fade countermeasures on a satellite-Earth link operating in an equatorial climate, with reference to broadcast applications," *IEE Proceedings — Microwaves, Antennas and Propagation*, Vol. 147, No. 5, 369–373, 2000.

[5] Budalal, A. A. H., M. R. Islam, K. Abdullah, and T. A. Rahman, "Modification of distance factor in rain attenuation prediction for short-range millimeter-wave links," *IEEE Antennas and Wireless Propagation Letters*, Vol. 19, No. 6, 1027–1031, Jun. 2020.

[6] Lin, S. H., "Dependence of rain-rate distribution on rain-gauge integration time," *The Bell System Technical Journal*, Vol. 55, No. 1, 135–141, Jan. 1976.

[7] Ong, J. T. and C. N. Zhu, "Effects of integration time on rain rate statistics for Singapore," in *Tenth International Conference on Antennas and Propagation (Conf. Publ. No. 436)*, Vol. 2, 273–276, Edinburgh, UK, 1997.

[8] Lee, J.-H., Y.-S. Kim, J.-H. Kim, and Y.-S. Choi, "Empirical conversion process of rain rate distribution for various integration time," in *2000 Asia-Pacific Microwave Conference. Proceedings (Cat. No. 00TH8522)*, Vol. 2, 1593–1597, Sydney, NSW, Australia, 2000.

[9] Jung, M.-W., I.-T. Han, M.-Y. Choi, J.-H. Lee, and J.-K. Pack, "Study on the empirical prediction of 1-min rain rate distribution from various integration time data," in *2007 Korea-Japan Microwave Conference*, 89–92, Naha, Japan, 2007.

[10] Fukuchi, H., "Integration time dependence of rainfall rate spatial correlation derived from radar rain map," in *2018 International Symposium on Antennas and Propagation (ISAP)*, 1–2, Busan, Korea (South), 2018.

[11] Rafiqul, I., M. Alam, A. K. Lwas, and S. Y. Mohamad, "Rain rate distributions for microwave link design based on long term measurement in Malaysia," *Indonesian Journal of Electrical Engineering and Computer Science*, Vol. 10, No. 3, 1023–1029, 2018.

[12] Moupfouma, F., "Point rainfall rate cumulative distribution function valid at various locations," *Electronic Letters*, Vol. 29, No. 17, 1993.

[13] Moupfouma, F. and O. D. Oyedum, "Recent advances in the global moupfoma model for tropical rain attenuation prediction," *IEEE Transactions on Antennas and Propagation*, Vol. 71, No. 3, 456–463, 2023.

[14] Moupfouma, F. and E. R. Martins, "Further modifications to the global moupfoma model for tropical rain attenuation prediction," in *PhotonIcs & Electromagnetics Research Symposium*, 234–241, Prague, Czech Republic, Jul. 2023.

[15] Moupfouma, F. and O. D. Oyedum, "Modifications to the global moupfoma model for improved rain attenuation prediction in tropical regions," *Radio Science*, Vol. 57, No. 3, 1–12, 2022.

[16] Chebil, J. and T. A. Rahman, "Development of 1 min rain rate contour maps for microwave application in Malaysia Peninsula," *Electronic Letters*, Vol. 35, No. 20, 1999.

[17] Crane, R. K., "Prediction of attenuation by rain," *IEEE Transaction on Communication*, Vol. COM-28, No. 9, 1717–1733, Sep. 1980.

[18] Ojo, J. S. and M. O. Ajewole, "Recent developments in the CRENE model for rain attenuation prediction," *IEEE Transactions on Wireless Communications*, Vol. 22, No. 5, 321–328, 2023.

[19] Rice, P. L. and R. K. Holmberg, "Recent developments in the CRENE model for rain attenuation prediction," *IEEE Transactions on Communications*, Vol. 21, No. 10, 1131–1136, 1973.

[20] Holmberg, J. and P. L. Rice, "Application of the Rice Holmberg model in tropical regions: Recent findings," *Journal of Atmospheric and Solar-Terrestrial Physics*, Vol. 235, 1–10, 2023.

[21] Holmberg, J. and P. L. Rice, "Revisiting the rice Holmberg model for rain attenuation prediction," *IEEE Transactions on Geoscience and Remote Sensing*, Vol. 59, No. 6, 4567–4578, 2021.

[22] Momin, M., M. M. Alam, M. M. H. Mahfuz, M. R. Islam, M. H. Habaebi, and K. Badron, "Prediction of rain attenuation on earth-to-satellite link using rain rate measurement with various integration times," in *2021 8th International Conference on Computer and Communication Engineering (ICCCE)*, 385–390, Kuala Lumpur, Malaysia, Jun. 2021.

[23] Marzuki, M., H. Hashiguchi, T. Shimomai, and W. L. Randeu, "Cumulative distributions of rainfall rate over Sumatra," *Progress In Electromagnetics Research M*, Vol. 49, 1–8, 2016.

[24] Obiyemi, O. O., J. Ojo, and T. S. Ibiyemi, "Performance analysis of rain rate models for microwave propagation designs over tropical climate," *Progress In Electromagnetics Research M*, Vol. 39, 115–122, 2014.

[25] Livieratos, S. N., Z. Ioannidis, S. Savaidis, S. Mitilineos, and N. Stathopoulos, "A new prediction method of rain attenuation along millimeter wave links based on a bivariate model for the effective path length and Weibull distribution," *Progress In Electromagnetics Research C*, Vol. 97, 29–41, 2019.

[26] Ulaganathen, K., T. B. A. Rahman, A. Y. Abdulrahman, and S. K. B. A. Rahim, "Comparative studies of the rain attenuation predictions for tropical regions," *Progress In Electromagnetics Research M*, Vol. 18, 17–30, 2011.

[27] Ghanim, M., M. Alhilali, J. Din, and H. Y. Lam, "Rain attenuation statistics over 5G millimetre wave links in Malaysia," in *2018 5th International Conference on Electrical Engineering, Computer Science and Informatics (EECSI)*, 266–269, Malang, Indonesia, 2018.

[28] ITU-R P.838-3, "Specific attenuation model for rain for use in prediction methods," Mar. 2005.